

1 **Biodegradation and photooxidation**  
2 **of phenolic compounds in soil - a**  
3 **compound-specific stable isotope**  
4 **approach**

5

6 Zacharias Steinmetz (1), Markus P. Kurtz (1), Jochen P. Zubrod (2), Armin H. Meyer (3), Martin Elsner  
7 (3,4), and Gabriele E. Schaumann (1)\*

8

9 (1) Institute for Environmental Sciences, Group of Environmental and Soil Chemistry, University of  
10 Koblenz-Landau, Fortstraße 7, 76829 Landau, Germany

11 (2) Institute for Environmental Sciences, Group of Ecotoxicology & Environment, University of  
12 Koblenz-Landau, Fortstraße 7, 76829 Landau, Germany

13 (3) Helmholtz Zentrum Muenchen, Institute of Groundwater Ecology, Ingolstädter Landstraße 1, 85764  
14 Neuherberg, Germany

15 (4) Institute of Hydrochemistry, Chair for Analytical Chemistry and Water Chemistry, Technical  
16 University of Munich, Marchioninistraße 17, 81377 Munich, Germany

17

18 \* Corresponding author: Gabriele E. Schaumann, e-mail: [schaumann@uni-landau.de](mailto:schaumann@uni-landau.de), Phone: +49 (0)  
19 6341 14 280-31571

## 20 **Abstract**

21 Phenolic compounds occur in a variety of plants and can be used as model compounds for investigating  
22 the fate of organic wastewater, lignin, or soil organic matter in the environment. The aim of this study  
23 was to better understand and differentiate mechanisms associated with photo- and biodegradation of  
24 tyrosol, vanillin, vanillic acid, and coumaric acid in soil. In a 29 d incubation experiment, soil spiked  
25 with these phenolic compounds was either subjected to UV irradiation under sterile conditions or to the  
26 native soil microbial community in the dark. Changes in the isotopic composition ( $\delta^{13}\text{C}$ ) of phenolic  
27 compounds were determined by gas chromatography–isotope ratio mass spectrometry and complemented  
28 by concentration measurements. Phospholipid-derived fatty acid and ergosterol biomarkers together with  
29 soil water repellency measurements provided information on soil microbial and physical properties.  
30 Biodegradation followed pseudo-first-order dissipation kinetics, enriched remaining phenolic  
31 compounds in  $^{13}\text{C}$ , and was associated with increased fungal rather than bacterial biomarkers. Growing  
32 mycelia rendered the soil slightly water repellent. High sample variation limited the reliable estimation  
33 of apparent kinetic isotope effects (AKIEs) to tyrosol. The AKIE of tyrosol biodegradation was  
34  $1.007 \pm 0.002$ . Photooxidation kinetics were of pseudo-zero- or first-order with an AKIE of  $1.02 \pm 0.01$   
35 for tyrosol, suggesting a hydroxyl-radical mediated degradation process. Further research needs to  
36 address  $\delta^{13}\text{C}$  variation among sample replicates potentially originating from heterogeneous reaction  
37 spaces in soil. Here, nuclear magnetic resonance or nanoscopic imaging could help to better understand  
38 the distribution of organic compounds and their transformation in the soil matrix.

## 39 **Highlights**

- 40 ⑩ Biodegradation of phenolic compounds was associated with increased fungal biomarkers
- 41 ⑩ Photooxidation of phenolic compounds was potentially catalyzed by hydroxyl radicals
- 42 ⑩ Dissipation kinetics could be described by a pseudo-zero order rate law
- 43 ⑩ High variation in  $\delta^{13}\text{C}$  between soil samples calls for further method development

44

## 45 **Keywords**

46 Polyphenols, allelochemicals, olive mill wastewater, soil fungi, stable isotopes, metabolic pathways

## 47 **1. Introduction**

48 Natural phenolic compounds occur in a variety of plants such as olives, grapes, or tea, and thus function  
49 as precursors for plant residues, lignin, soil organic matter (SOM), or organic wastewater (Justino et al.,  
50 2010; Siqueira et al., 1991). This makes phenolic compounds, specifically phenolic alcohols and  
51 hydroxycinnamic acid derivatives, an important group of model compounds for facilitating a better  
52 understanding of the environmental fate and turnover processes of plant residues in soil (Glaser, 2005).  
53 Such fate studies become particularly relevant when plant pomaces or organic wastewater is applied to  
54 soil.

55 Olive mill wastewater (OMW), for instance, is particularly rich in phenolic compounds and serves as a  
56 natural fertilizer in the Mediterranean due to its high content in potassium, manganese, and calcium  
57 (Barbera et al., 2013). While low concentrations of phenolic compounds may repel pests or stimulate  
58 beneficial organisms, phenolic compounds can adversely affect soil fauna when released extensively  
59 (Kurtz et al., 2015; Peikert et al., 2015). In semi-arid and Mediterranean climates, the fate of phenolic  
60 compounds originating from OMW largely depends on the application season and the time passed since  
61 the last application, ranging from not any to complete dissipation after 6–18 months (Steinmetz et al.,  
62 2015). Buchmann et al. (2015) suggested that the transformation of phenolic OMW constituents may  
63 involve three subprocesses, including (1) mineralization of easily accessible phenolic compounds, (2)  
64 transformation of more recalcitrant phenolic substances, and (3) immobilization or incorporation of  
65 phenolic compounds into SOM. However, current understanding remains contrasting in terms of the  
66 extent bacteria and fungi may be involved in biodegradation of phenolic OMW constituents under various  
67 environmental conditions (Laor et al., 2011; Peikert et al., 2017). In addition, OMW spread on topsoil  
68 and exposed to sunlight has been assumed to induce photooxidation and polymerization of phenolic  
69 compounds, potentially rendering soil water repellent (Tamimi et al., 2016).

70 The objective of our study was to better understand natural biodegradation and photooxidative processes  
71 of phenolic compounds in soil to identify unique characteristics of both transformation mechanisms in

72 the field, for instance, after an OMW application. Based on the assumptions by Tamimi et al. (2016) and  
73 Peikert et al. (2017), we hypothesized that (1) natural biodegradation of phenolic compounds is more  
74 facilitated by fungi rather than bacteria and that (2) differences in dissipation kinetics of biological and  
75 photooxidative processes lead to distinct isotope fractionation of phenolic compounds during  
76 degradation.

77 In order to investigate this, we spiked an olive orchard soil with four phenolic compounds typically found  
78 in OMW, namely tyrosol, vanillin, vanillic acid, and coumaric acid (Buchmann et al., 2015; Justino et  
79 al., 2010), and let them be degraded for 29 d either by the native soil microbial community in the dark or  
80 by ultraviolet (UV) irradiation under sterile conditions. The duration of the experiment was chosen based  
81 on previous studies that found more than 80% of OMW-derived phenolic compounds degraded within  
82 the first 30 days after application (Buchmann et al., 2015; Peikert et al., 2017). To track the degradation  
83 of phenolic compounds, we analyzed changes in their isotopic carbon composition ( $\delta^{13}\text{C}$ ) using gas  
84 chromatography–isotope ratio mass spectrometry (GC–IRMS; Elsner, 2010). Compound-specific carbon  
85 stable isotope analysis has been proven useful to detect abiotic or biotic transformation reactions of  
86 organic compounds based on their specific isotope fractionation during degradation (Elsner et al., 2005).  
87 However, making phenolic compounds amenable for routine GC–IRMS measurements requires prior  
88 derivatization to decrease their polarity. Therefore, we first developed and validated a derivatization  
89 procedure suitable for subsequent GC–IRMS measurements. Our analyses were complemented with soil  
90 respiration measurements to assess the overall soil metabolic activity. Ergosterol and phospholipid-  
91 derived fatty acid (PLFA) biomarkers were used as indicators for fungal biomass and soil microbial  
92 community composition, respectively. Water drop penetration time (WDPT) measurements served as a  
93 proxy for soil water repellency.

## 94 **2. Materials and methods**

### 95 ***2.1. Experimental setup***

96 Incubation conditions were aimed to reflect average field conditions of a typical OMW application  
97 scenario, in an olive orchard in the Northern Negev, Israel, during spring (March to May). Incubation  
98 temperature and relative humidity were set to  $22 \pm 1$  °C and  $32 \pm 1$  %, respectively. A sieved Israeli olive

99 orchard topsoil (0–10 cm, <2 mm mesh) as previously used elsewhere (Buchmann et al., 2015;  
100 Steinmetz et al., 2015) served as reference soil. Briefly, the fine soil contained 56 % sand, 13 % silt, and  
101 31 % clay (loessial sandy clay loam) with a bulk density of 1.17 g cm<sup>-3</sup> and an effective cation exchange  
102 capacity of 33 mmol<sub>c</sub> kg<sup>-1</sup> at a soil pH<sub>H2O</sub> of 7.9. Organic and inorganic carbon were 5 ± 1 g kg<sup>-1</sup> and  
103 27 ± 6 g kg<sup>-1</sup>, respectively, with a bulk δ<sup>13</sup>C of -8.5 ‰.

104 The incubation experiment was set up in triplicates by transferring each 10 g of air-dried soil into screw  
105 cap glass jars equipped with a 0.1 μm air filter (99.8 % bacterial filtration efficiency; EN 14683, 2014)  
106 and a septum port for sterile injections. After a 14-d preincubation period in the dark, one subset of  
107 incubation jars was spiked with the phenolic compounds to initiate biodegradation by the native soil  
108 microbial community. The spiking solution contained each 10 mg of tyrosol, vanillin, vanillic acid, and  
109 *m*-coumaric acid dissolved in 500 μL of a 1:1 mixture of methanol and ultrapure water (see  
110 supplementary material S1 for purities and suppliers of all chemicals used in this study). With that, a  
111 nominal content of 1 g kg<sup>-1</sup> of each phenolic compound in soil was obtained, which reflects typical  
112 contents of phenolic compounds in topsoil directly after OMW application (Buchmann et al., 2015; Sierra  
113 et al., 2001). Another subset of preincubated soil was sterilized by autoclaving at 121 °C for 20 min prior  
114 to spiking with phenolic compounds. After two days, the soil was autoclaved a second time to prevent  
115 potential recolonization from spores. During incubation, soils were kept sterile and irradiated with UV  
116 light (7 W m<sup>-2</sup> UVA and 0.02 W m<sup>-2</sup> UVB, CLEO Performance N, Philips, Amsterdam, Netherlands) for  
117 16 h per day to trigger photooxidative degradation. In addition to these two treatments, sterilized soil  
118 spiked with phenolic compounds and incubated in the dark (without UV) was used to quantify sorption  
119 or complexation processes. Incubation jars filled with plate-count agar (5 g L<sup>-1</sup> peptone, 2.5 g L<sup>-1</sup> yeast  
120 extract, 1 g L<sup>-1</sup> glucose, 15 g L<sup>-1</sup> agar, pH 7.0) were used to verify sterility by visual absence of colony-  
121 forming units. Sterilized and non-sterilized soils treated with a clean methanol–water mixture free of  
122 phenolic compounds served as controls.

123 During the experiment, the soil matrix potential was kept at -63 kPa (pF = 2.8) by tempering weight  
124 losses of incubation jars with the addition of ultrapure water. The soil was sampled by sacrificing  
125 incubation jars (*n* = 6) at days 0, 1, 2, 4, 8, 15 and 29. All samples were freeze-dried at a constant weight  
126 and stored at -20 °C for further analyses.

## 127 **2.2. Extraction and quantification of phenolic compounds**

128 Phenolic compounds were extracted from 2 g of soil with 10 mL of methanol for 24 h at 400 rpm in an  
129 orbital shaker. Preliminary experiments showed that this extraction procedure yielded highest and most  
130 reproducible recoveries compared to accelerated solvent extraction, microwave-induced extraction,  
131 ultrasonic extraction, and sequential extraction with hexane and methanol (see supplementary material  
132 S2). After sedimentation, supernatants were filtered through 0.45  $\mu\text{m}$  syringe filters.

133 Phenolic compounds were separated by high-performance liquid chromatography (HPLC, Series 1200,  
134 Agilent, Santa Clara, USA) on a  $\text{C}_{18}$  reversed-phase column (Nucleodur C18 Pyramid, 5  $\mu\text{m}$ , Macherey-  
135 Nagel, Düren, Germany). The mobile phase consisted of acidified ultrapure water (0.2 % formic acid)  
136 and a gradually increasing percentage of acetonitrile (5 % for 5 min, 5 to 40 % for 13 min; 40 to 90 %  
137 for 6 min with a final 1-min hold; 0.8  $\text{mL min}^{-1}$  total flow). Phenolic compounds were quantified with a  
138 UV detector at 280 nm against external standards. All chromatograms were screened manually for  
139 unidentified peaks to be investigated by gas chromatography–mass spectrometry (GC–MS) as described  
140 in the following section.

## 141 **2.3. Compound-specific stable isotope analysis of phenolic compounds**

142 Prior to GC–IRMS analysis, phenolic compounds needed to be derivatized into their respective ethers  
143 and esters (Elsner et al., 2012; Reinnicke et al., 2010). For that, standard test mixtures of the four phenolic  
144 compounds (10–500  $\text{mg L}^{-1}$ ) with and without soil matrix were prepared and their susceptibility to  
145 various derivatization agents was evaluated. These were trimethylsulfonium hydroxide (TMSH)  
146 according to a method by Reinnicke et al. (2010), trimethylanilinium hydroxide (TMAH) based on  
147 Rompa et al. (2004),  $\text{BF}_3$  (Maier et al., 2014; Meier-Augenstein, 1997), and a Purdie methylation with  
148  $\text{CH}_3\text{I}$  modified by Lehmann et al. (2017). Derivatization agents were added in varying molar excess (10–  
149 400 fold) and phenolic standard solutions were left for either 30 or 60 min at 30, 40, 60, and 80  $^\circ\text{C}$ ,  
150 respectively, in hermetically crimped vials (ND11 with aluminum seal and butyl/PTFE septum, VWR,  
151 Darmstadt, Germany). Phenolic derivatives were identified and their reaction yield was checked by GC–  
152 MS (GC Trace Ultra + DSQII-MSD, Thermo Fisher Scientific, Bremen, Germany). Specifically, 0.5–  
153 2.5  $\mu\text{L}$  sample volume were injected into various inlet liners either splitless at constant temperature (150,

154 200, or 250 °C) or by purging excess solvent for 0.1 min (80 mL min<sup>-1</sup> split flow) prior to rapid injector  
155 heating with a 14 °C s<sup>-1</sup> ramp from 100 to 250 °C. Tested liner types included straight, tapered, and  
156 baffled glass liners, stainless steel as well as glass liners filled with glass wool or a carbofrit. Optionally,  
157 carbofrit liners were packed with 250 µm or 400–600 µm silanized glass beads (see supplementary  
158 material S1 for materials). The analytes were separated on a 60 m × 0.25 mm capillary column (5 %  
159 phenyl-arylene, 95 % dimethylpolysiloxane, 0.25 µm film thickness, ZB-5MS, Phenomenex,  
160 Aschaffenburg, Germany) equipped with 2-m deactivated fused silica guard column (Phenomenex,  
161 Aschaffenburg, Germany) in order to avoid film decomposition by derivatization agents. The oven  
162 program was adjusted by optimizing chromatographic resolution  $R_s$  as defined in Equation 1. Therein,  
163  $t_{R1}$  and  $t_{R2}$  [min] are the retention times of adjacent peaks, and  $w_{b1}$  and  $w_{b2}$  [min] are corresponding peak  
164 widths taken from integration thresholds (Meyer et al., 2015).

$$165 \quad R_s = 2 \cdot \frac{t_{R2} - t_{R1}}{w_{b2} + w_{b1}} \quad (1)$$

166 If applicable, methods producing sufficiently high signal intensities were examined for signal stability  
167 and linearity by repeatedly measuring standard series of phenolic model compounds both via GC–MS  
168 and GC–IRMS (Trace GC Ultra with GC IsoLink coupled to a ConFlo IV and Delta V Advantage IRMS,  
169 Thermo Fisher Scientific, Bremen, Germany). In order to increase reproducibility, test mixtures were  
170 spiked with 2-naphthol as internal standard (IS) for tyrosol and vanillin derivatives. Vanillic acid and  
171 coumaric acid derivatives were IS-corrected with biphenyl-2-carboxylic acid. The ISs were selected for  
172 their structural similarity to the analytes while ensuring their absence in natural soil and sufficient  
173 chromatographic separation.

174 After chromatographic separation, phenolic derivatives were combusted to CO<sub>2</sub> at 1000 °C in a freshly  
175 oxidized CuO–NiO reactor tube (Thermo Fisher Scientific, Bremen, Germany). Reactor tube reoxidation  
176 was performed after each measurement by flushing oxygen over the CuO–NiO catalyst for 20 s followed  
177 by a 120 s He (grade 5.0) vent. The isotopic composition of CO<sub>2</sub> was converted by software (Isodat 3.0,  
178 Thermo Fisher Scientific, Bremen, Germany) into compound-specific  $\delta^{13}\text{C}$  relative to Vienna Pee Dee  
179 Belemnite and in-house references (Equation 2).

$$180 \quad \delta^{13}\text{C} = \frac{{}^{13}\text{C}/{}^{12}\text{C}_{\text{Sample}} - {}^{13}\text{C}/{}^{12}\text{C}_{\text{Reference}}}{{}^{13}\text{C}/{}^{12}\text{C}_{\text{Reference}}} \quad (2)$$

181 Derivatization introduces foreign carbon atoms into the phenolic molecule, changing the  $\delta^{13}\text{C}$  of the  
182 analyte. Therefore, phenolic derivatives were corrected with bracketing standards of known isotopic  
183 composition as verified by elemental analyzer–isotope ratio mass spectrometry (EA–IRMS, Flash HT  
184 with SmartEA coupled to the same IRMS system, Thermo Fisher Scientific, Bremen, Germany) using  
185 Equation 3 (Maier et al., 2014);  $n$  is the number of carbon atoms in the respective molecule.

$$186 \quad \delta^{13}\text{C}_{\text{Sample}} = n_{\text{Derivative, Standard}} \cdot \left( \frac{\delta^{13}\text{C}_{\text{Derivative, Sample}} - \delta^{13}\text{C}_{\text{Derivative, Standard}}}{n_{\text{Standard}}} \right) + \delta^{13}\text{C}_{\text{Standard}} \quad (3)$$

187 In addition,  $\delta^{13}\text{C}$  values of phenolic derivatives were corrected with the  $\delta^{13}\text{C}$  of their respective IS to  
188 reduce potential isotope shifts from chromatographic effects or incomplete combustion in the reactor  
189 tube. IS correction was performed by subtracting the  $\delta^{13}\text{C}$  of the IS determined by EA–IRMS from those  
190 obtained from GC–IRMS measurements. This difference was then applied to the  $\delta^{13}\text{C}$  values of the  
191 sample.

192 For method validation, we purchased a second set of phenolic model compounds from different suppliers  
193 as a reference (see supplementary material S1) and determined their  $\delta^{13}\text{C}$  composition both by EA–IRMS  
194 and GC–IRMS after IS-correction. At last, the GC–IRMS method was applied to the soil samples of our  
195 incubation experiment and the variation in  $\delta^{13}\text{C}$  within sample replicates was evaluated.

#### 196 ***2.4. Soil respiration, biomarkers, and water repellency***

197 Soil respiration was recorded at days 0 and 29 of the incubation study using the MicroResp method  
198 without substrate addition (Campbell et al., 2003). To this end, four aliquots of sample were transferred  
199 into wells of a deep well microtiter plate. The soil was equilibrated at 20 °C for 16 h to reduce artifacts  
200 from manual soil perturbation. Subsequently, the well plate was covered air-tight with a detection  
201 microtiter plate filled with CO<sub>2</sub>-sensitive indicator agar (12.5 mg L<sup>-1</sup> cresol red, 150 mM KCl, 2.5 mM  
202 NaHCO<sub>3</sub>) and incubated for 25 h. After incubation, the color change of the indicator was quantified with  
203 a plate reader (Infinite M200, TECAN, Männedorf, Switzerland) at 572 nm.

204 Fungal biomass at days 0 and 29 was estimated from free ergosterol contents extracted by physical  
205 disruption (Gong et al., 2001). Accordingly, 5 mL of methanol were added to 1 g of freeze-dried soil  
206 together with 1 g of acid-cleaned glass beads (equivalent amount of beads with 150–250 μm and 700–



207 1000 µm diameter, Carl Roth, Karlsruhe, Germany). The suspension was agitated for 1 h at 400 rpm in  
208 an orbital shaker. Suspended particles were allowed to sediment and the supernatants were filtered  
209 through 0.45 µm syringe filters. After extraction, ergosterol was eluted isocratically (1 mL min<sup>-1</sup>  
210 methanol) at 33 °C via HPLC equipped with a C<sub>18</sub> reversed-phase column (LiChrospher 100 RP 18-5µ,  
211 CS Chromatographie-Service, Langerwehe, Germany) and quantified with a UV detector at 282 nm.

212 In order to assess changes in the composition of the soil microbial community, freeze-dried soils sampled  
213 at the first and last day of the incubation experiment (day 0 and 29) were analyzed for PLFA biomarkers  
214 according to Bligh and Dyer (1959) and Butte (1983). In brief, phospholipids were extracted from 2 g  
215 soil using a mixture of 2 mL chloroform, 4 mL methanol, and 1.6 mL phosphate buffer. Extracts were  
216 agitated for 1 h in an overhead shaker (16 rpm) and purified via solid phase extraction (SPE) with a  
217 modified polar polystyrene-divinylbenzene copolymer (Chromabond, Macherey-Nagel, Düren,  
218 Germany). Phospholipids were transesterified with TMSH (0.25 M in methanol). The resulting fatty acid  
219 methyl esters (FAMES) were quantified by gas chromatography with flame ionization detector (CP-3800,  
220 Varian, Darmstadt, Germany). External standards for FAME quantification were *i*15:0 and *i*17:0 for  
221 Gram<sup>+</sup> bacteria, 16:1 $\omega$ 7c, 18:1 $\omega$ 9c and 18:1 $\omega$ 7c for Gram<sup>-</sup> bacteria, 16:1 $\omega$ 5c for mycorrhiza, and  
222 18:2 $\omega$ 6c for fungi (Zelles, 1999). Deuterated 18:0 and deuterated 14:0 were used as IS.

223 Soil water repellency potentially induced by polymerization of phenolic compounds was assessed by  
224 taking WDPTs on fresh soil at day 0 and 29. To this end, droplets of deionized water (100 µL) were  
225 placed onto the soil surface and the time to complete penetration of each droplet was determined. WDPTs  
226 were classified according to Bisdom et al. (1993).

## 227 **2.5. Data evaluation**

228 Data processing and statistical analyses were performed using R (version 3.5.1). All results are presented  
229 as mean  $\pm$  95 % confidence interval (CI). Limits of detection (LODs) and limits of quantification (LOQs)  
230 were calculated from blank measurements in accordance with German standard DIN 32645 (2008) as  
231 implemented in the R package “envalysis” (version 0.3.3, code publicly available from  
232 <https://doi.org/cn74>). Changes in phenolic compounds, soil biomarkers, respiration, and water repellency

233 during incubation were statistically evaluated by 95 % CI testing (Wheeler et al., 2006) as implemented  
234 in the R package “drc”.

235 Dissipation kinetics were assessed by fitting zero-order (Equation 4) and first-order rate equations  
236 (Equation 5) to phenolic soil contents  $c_t$  [mg kg<sup>-1</sup>] changing with incubation time  $t$  [d];  $c_0$  is the initial  
237 phenolic content [mg kg<sup>-1</sup>] at time  $t = 0$  [d].  $k_{\text{zero}}$  [mg kg<sup>-1</sup> d<sup>-1</sup>] and  $k_{\text{first}}$  [d<sup>-1</sup>] are the dissipation rates.

$$238 \quad c_t = c_0 - k_{\text{zero}} \cdot t \quad (4)$$

$$239 \quad c_t = c_0 \cdot e^{-k_{\text{first}} \cdot t} \quad (5)$$

240 The resulting regression models were evaluated for their goodness of fit using corrected Akaike  
241 information criteria (AICs, from R package “MuMIn”) and adjusted  $R^2$ . 95 % CI testing of prediction  
242 intervals was used to check for significant differences between the expected rate equation and its  
243 potentially better fitting alternative (Wheeler et al., 2006).

244 In addition, ln-transformed linear models were used to estimate isotope enrichment  $\varepsilon$  [‰] occurring  
245 during degradation of phenolic compounds as defined by the Rayleigh equation (Equation 6). The  
246 Rayleigh equation relates isotope ratios at incubation time  $t$  ( $\delta^{13}\text{C}_t$  [‰]) with respect to initial  $\delta^{13}\text{C}_0$  [‰]  
247 with the fraction  $c_t/c_0$  of remaining parent compound (Elsner, 2010).

$$248 \quad \ln\left(\frac{\delta^{13}\text{C}_t + 1}{\delta^{13}\text{C}_0 + 1}\right) = \varepsilon \cdot \ln\left(\frac{c_t}{c_0}\right) \quad (6)$$

249 On this basis, Equation 7 was used to estimate a compound-averaged apparent kinetic isotope effect  
250 (AKIE) by relating  $\varepsilon$  to the number of carbon atoms  $n$  in each phenolic compound (Elsner et al., 2005).

$$251 \quad \text{AKIE} \approx (1 + n \cdot \varepsilon)^{-1} \quad (7)$$

252 The AKIE comprises isotope effects of all steps of a reaction chain. A rate-determining but hardly  
253 fractionating step such as formation of an enzyme–substrate complex could mask the intrinsic kinetic  
254 isotope effect of the bond-changing reaction typically used to identify a certain reaction mechanism. In  
255 such cases, the AKIE is smaller than expected which needs to be taken into account when interpreting  
256 results (Elsner et al., 2005).

257

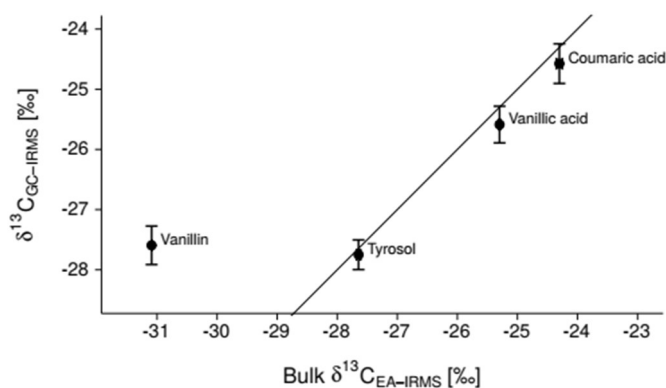
## 258 **3. Results and discussion**

### 259 **3.1. Development and validation of a derivatization method to analyze phenolic** 260 **model compounds by GC–IRMS**

261 Off-line derivatization with TMSH at more than 100-fold excess for 30 min at 40 °C followed by splitless  
262 injection of 1.5 µL into a 250 °C glass bead liner produced best results in terms of  $\delta^{13}\text{C}$  signal sensitivity  
263 and reproducibility. Stable  $\delta^{13}\text{C}$  values were obtained for peak amplitudes greater than 500 mV. Multiple  
264 injections of phenolic standard mixtures ( $n = 32$ ) into the GC–IRMS resulted in a precision of  $<0.19\text{‰}$   
265 measurement variation (95 % CI, see supplementary material S3 for figures). Baseline separated peaks  
266 with a chromatographic resolution  $R_s \geq 2$  (Meyer et al., 2015) were achieved for tyrosol, vanillic acid,  
267 and coumaric acid derivatives when applying the following GC oven program: 80 °C (1 min hold),  
268 10 °C  $\text{min}^{-1}$  ramp to 140 °C (5 min hold), 2 °C  $\text{min}^{-1}$  ramp to 180 °C, and a final 25 °C  $\text{min}^{-1}$  ramp to  
269 300 °C (1 min hold). The vanillin derivative interfered with a derivatization by-product ( $R_s = 1$ ) and peaks  
270 remained chromatographically inseparable from one another when extending the oven program.

271 EA–IRMS measurements showed that bulk  $\delta^{13}\text{C}$  values of the second set of phenolic reference  
272 compounds used for method validation were about 1 ‰ lighter than  $\delta^{13}\text{C}$  values of the standard mixture  
273 used for standard bracketing (coumaric acid was by 0.16 ‰ heavier; see supplementary material S3 for  
274 comparisons). Compound-specific  $\delta^{13}\text{C}$  values obtained by GC–IRMS measurements after correction  
275 with bracketing standards and IS accurately reproduced EA–IRMS measurements of tyrosol, vanillic  
276 acid, and coumaric acid reference compounds (Figure 1). GC–IRMS measurement uncertainties were  
277 typically below 0.3 ‰. Only vanillin deviated from the identity line by 3 ‰ which was most likely due  
278 to the insufficient chromatographic separation. For this reason, vanillin was excluded from further isotope  
279 analyses.

280



281 *Figure 1: Validation of GC-IRMS measurements against EA-IRMS measurements of a phenolic reference*  
 282 *mixture, the solid line is the 1:1 line; error bars indicate 95 % CIs (the variability of bulk  $\delta^{13}C_{EA-IRMS}$*   
 283 *values was < 0.05 ‰)*

284

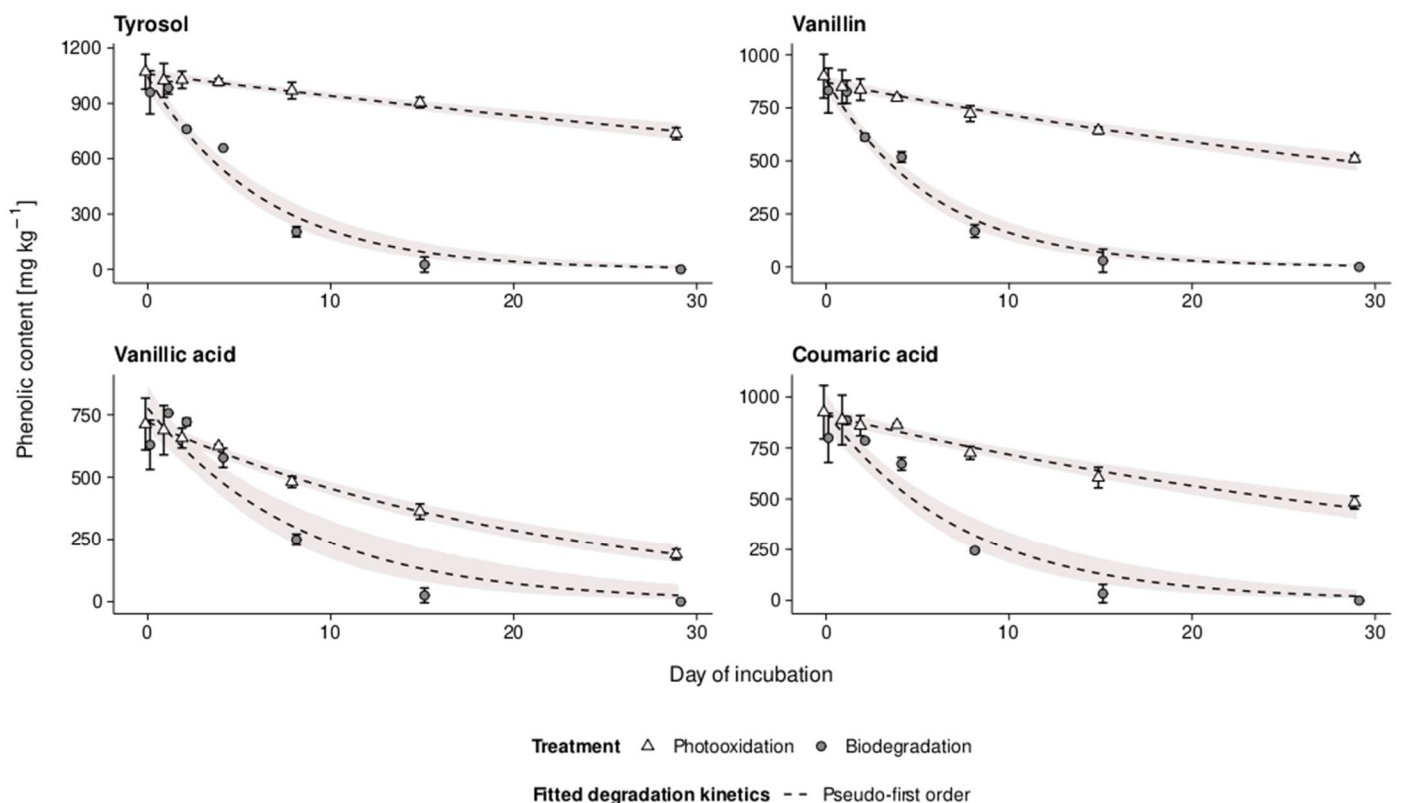
285 Our preferred GC-IRMS procedure is in line with findings by Reinnicke et al. (2010), who established a  
 286 GC-IRMS method for the compound-specific stable isotope analysis of (4-chloro-2-  
 287 methylphenoxy)acetic acid and bentazone after derivatization with TMSH. The authors stressed the  
 288 importance of using excess TMSH in order to avoid irreproducible derivatization-induced isotope shifts  
 289 potentially originating from spatial isolation of analytes and derivatization agent in the porous space of  
 290 the glass bead liner (Reinnicke et al., 2010). This effect may also explain the analyte carry-over we  
 291 observed unless we added a cleaning run after every fifth sample injection. Unpacked liners generally  
 292 performed worse in terms of reproducibility. Liners packed with glass wool showed even higher carry-  
 293 over effects than glass bead liners.

294 In comparison to TMSH, derivatization with TMAH and  $BF_3$  resulted in lower measurement sensitivities  
 295 due to a substantial background noise from phenyl and fluoric mass fragments. The low turnover of the  
 296 modified Purdie reaction rendered the detection of phenolic compounds at concentrations < 200 mg L<sup>-1</sup>  
 297 impossible. Lehmann et al. (2017) initially developed and applied the method for  $\delta^{18}O$  of carbohydrates  
 298 in the g L<sup>-1</sup> range. Since we expected analyte concentrations in our experiment to be 2–3 orders of  
 299 magnitude lower than the concentrations used by Lehmann et al. (2017), derivatization of phenolic  
 300 compounds with TMSH and hot injection into a glass bead liner was the superior method for our  
 301 experiment, and thus used for all further GC-IRMS analyses. After correction with bracketing standards

302 and IS, multiple injections of the same sample were both precise and accurate with deviations smaller  
 303 than 0.3 ‰ (see above).

### 304 3.2. Tracking the degradation of phenolic compounds

305 In non-spiked control soils, phenolic contents were generally below the respective LODs of 2–  
 306 123  $\mu\text{g kg}^{-1}$  (see supplementary material S3). Soils spiked with phenolic compounds had initial contents  
 307 of 627–1070  $\text{mg kg}^{-1}$  (Figure 2), which generally reflected their recovery rates from soil (see  
 308 supplementary material S2). In sterilized soil incubated in the dark, these initial levels decreased by about  
 309 20 % from day 0 to day 29 of the incubation experiment (see supplementary material S4). This may be  
 310 explained by sorption of hydroxy, carbonyl (vanillin only), or carboxylic moieties (vanillic acid and  
 311 coumaric acid) of phenolic compounds to clay minerals or SOM (Buchmann et al., 2015), complexation  
 312 with metal ions, or manganese-catalyzed polymerization (Gianfreda et al., 2006).



313 Figure 2: Dissipation kinetics of phenolic model compounds (mean  $\pm$  95 % CI) in soil subjected either to  
 314 photooxidation or biodegradation for 29 d; gray overlays indicate 95 % confidence bands of model fits

315 When subjected to UV-irradiation, phenolic contents decreased to 26–69 % of their initial content after  
 316 29 d of incubation. Photodegradation kinetics were in the best agreement with a first-order rate law (adj.

317  $R^2 \geq 0.849$ , Table 1), with vanillic acid being photodegraded the fastest while tyrosol and vanillin were  
 318 most recalcitrant. Except for vanillic acid, however, the differences to alternative zero-order models were  
 319 marginal and statistically insignificant (95 % CI testing, see supplementary material S5 for diagnostic  
 320 plots). Therefore, both models described the dissipation of tyrosol, vanillin, and coumaric acid equally  
 321 well. However, photodegradation reactions often follow first-order dissipation kinetics since they may  
 322 not only depend on the number of photons activating a compound for reaction but also on the compound  
 323 concentration. If rate-limiting, the presence of other reactants such as photocatalysts may even result in  
 324 dissipation kinetics of higher order (Schwarzenbach et al., 2016).

325

326 *Table 1: Dissipation rates with their respective standard error, adjusted  $R^2$  and AIC of the best-fitting*  
 327 *degradation models depicted in Figure 1*

| Compound      | Photooxidation                 |            |       | Biodegradation                 |            |       |
|---------------|--------------------------------|------------|-------|--------------------------------|------------|-------|
|               | $k_{first}$ [d <sup>-1</sup> ] | adj. $R^2$ | AIC   | $k_{first}$ [d <sup>-1</sup> ] | adj. $R^2$ | AIC   |
| Tyrosol       | 0.01 ± 0.01                    | 0.849      | 226.1 | 0.16 ± 0.02                    | 0.956      | 240.9 |
| Vanillin      | 0.02 ± 0.01                    | 0.895      | 224.9 | 0.17 ± 0.02                    | 0.965      | 229.6 |
| Vanillic acid | 0.05 ± 0.01                    | 0.945      | 225.8 | 0.12 ± 0.02                    | 0.891      | 248.4 |
| Coumaric acid | 0.02 ± 0.01                    | 0.869      | 238.2 | 0.13 ± 0.02                    | 0.923      | 248.2 |

328 *see supplementary material S5 for alternative zero-order models*

329

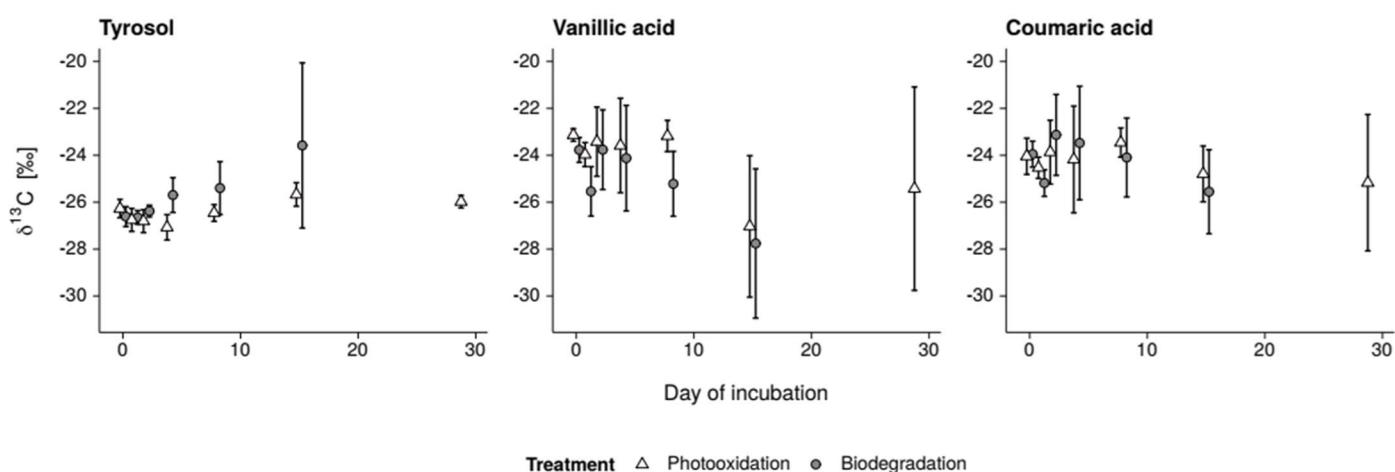
330 In non-sterilized soil incubated in the dark, phenolic contents remained constant in the first two days of  
 331 incubation, followed by complete dissipation (<LODs) towards the end of the incubation period.  
 332 Biodegradation kinetics were described best by a first-order rate law (adj.  $R^2 \geq 0.891$ ) with vanillic acid  
 333 degrading most slowly while vanillin was degraded the fastest. Alternative zero-order rate equations had  
 334 a lower goodness of fit that differed significantly from the expected first-order rate law (95 % CI testing,  
 335 see supplementary material S5). Deviations from the first-order rate law were found for vanillic acid and  
 336 coumaric acid, whose contents increased at day 2 before decreasing like all other phenolic compounds.  
 337 Buchmann et al. (2015) observed similar lag times for coumaric acid and caffeic acid. The authors argued  
 338 that various phenolic compounds may be biologically transformed into one another. This particularly  
 339 applies to vanillin which is known to be readily oxidized to vanillic acid by various soil microbes (Neilson

340 and Allard, 2008). Additionally, vanillic and coumaric acid sorbed to SOM may have been remobilized  
 341 by soil microbes prior to biodegradation. However, apart from vanillic acid, no further metabolites were  
 342 detected via HPLC to be identified by GC–MS. This may be attributed to the rapid metabolization of  
 343 phenolic acids into small, diverse aliphatic compounds no longer amenable to the UV detector of the  
 344 HPLC or scanning GC–MS (Blum and Shafer, 1988).

### 345 3.3. Changes in stable isotope ratios of phenolic compounds during degradation

346 Initial  $\delta^{13}\text{C}$  values of tyrosol, vanillic acid, and coumaric acid at day 0 of the incubation experiment were  
 347  $-26.4 \pm 0.3 \text{ ‰}$ ,  $-23.5 \pm 0.4 \text{ ‰}$ , and  $-24.0 \pm 0.4 \text{ ‰}$ , respectively (Figure 3). During biodegradation,  
 348 tyrosol became enriched in  $^{13}\text{C}$  by about 3.0 ‰. However, sample variation both between and within  
 349 sample replicates increased to  $\pm 3.5 \text{ ‰}$  towards the end of the incubation experiment at day 15 (see  
 350 supplementary material S3 comparisons in sample variation). This variation led to a moderate goodness  
 351 of fit (adj.  $R^2 = 0.732$ ,  $p < 0.001$ ) for the estimation of  $\epsilon = -0.9 \pm 0.3 \text{ ‰}$ . The corresponding AKIE was  
 352  $1.007 \pm 0.002$ . In contrast, vanillic acid was depleted by about 4.0 ‰ with 3.2 ‰ sample variation at day  
 353 15. This resulted in an inverse isotope effect with a derived  $\epsilon$  of  $1.7 \pm 0.7 \text{ ‰}$  and an associated AKIE of  
 354  $0.987 \pm 0.005$  (adj.  $R^2 = 0.599$ ,  $p < 0.001$ ). For coumaric acid, changes in  $\delta^{13}\text{C}$  were small and indistinct  
 355 with respect to sample variation ( $\epsilon = 0.3 \pm 0.5 \text{ ‰}$ , AKIE =  $0.997 \pm 0.005$ , adj.  $R^2 = 0.042$ ,  $p = 0.212$ ).

356



357 Figure 3:  $\delta^{13}\text{C}$  of phenolic model compounds (mean  $\pm$  95 % CI) during degradation; vanillin was omitted  
 358 due to unsuccessful method validation

359

360 During photooxidation,  $\delta^{13}\text{C}$  values of dissipating tyrosol varied only by 0.3–0.5 ‰ at each sampling day  
361 but remained at a relatively constant level of –25.7 to –27.1 ‰ during incubation. The estimated AKIE  
362 was  $1.02 \pm 0.01$  ( $\epsilon = -3 \pm 2$  ‰), however, with a considerably worse goodness of fit (adj.  $R^2 = 0.264$ ,  $p$   
363  $= 0.010$ ) compared to biodegradation. For both vanillic acid and coumaric acid, no clear isotope effects  
364 were found considering sample variations of up to 4.3 ‰. This resulted in adj.  $R^2 < 0.105$  and  $p > 0.084$ ,  
365 thereby inflating errors for the estimation of  $\epsilon$  and AKIEs.

366 Although precision and accuracy of replicate standard measurements were within acceptable limits  
367 ( $< 0.3$  ‰, see above) and comparable to other compound-specific stable isotope analyses (Maier et al.,  
368 2014; Reinnicke et al., 2010), the  $\delta^{13}\text{C}$  variation of soil sample replicates was about 10 times higher. Such  
369 high variations have been similarly observed by Dungait et al. (2008) who studied the isotopic carbon  
370 composition of phenolic lignin moieties in soil. Due to the heterogeneous nature of soil, substrates are  
371 often spatially separated from decomposers or other reaction agents. Moreover, hydroxy or carboxylic  
372 moieties of phenolic compounds easily sorb to SOM or clay minerals (Sierra et al., 2007) as indicated by  
373 a slight decrease of phenolic compounds incubated in the dark after sterilization. This suggests that  
374 distribution processes and transformation reactions in soil are likely to proceed nonuniformly in  
375 dependence of the sorption potential of an organic compound. With that, heterogeneous reaction spaces  
376 may form and lead to irregular isotope fractionation during compound degradation. Moreover, organic  
377 soil constituents can easily cause interferences in  $\delta^{13}\text{C}$  measurements, for instance, due to incomplete  
378 combustion of phenolic compounds in the combustion interface of the GC–IRMS. Follow-up studies  
379 should aim at disentangling the potential effects of soil matrix on changes in  $\delta^{13}\text{C}$ , for example, by  
380 analysis compound degradation in the presence and absence of different soils.

### 381 **3.4. Soil water repellency and biological activity**

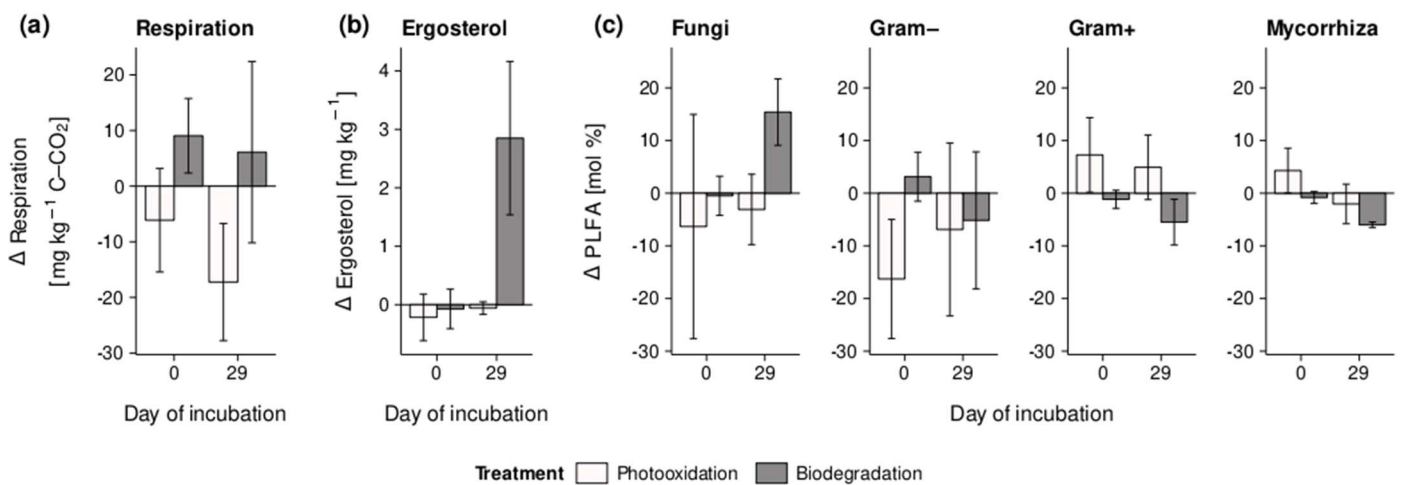
382 The 29-d incubation experiment considerably influenced soil water repellency, soil respiration as well as  
383 ergosterol and PLFA biomarkers (Figure 4). For reference, control soil without phenolic compounds was  
384 generally classified as wettable ( $< 5$  s WDPT) according to Bisdom et al. (1993). Photooxidation of  
385 phenolic compounds did not change the wetting behavior of the topsoil. Interestingly though, WDPTs  
386 increased to  $60 \pm 80$  s after 29 d of biodegradation of phenolic compounds, indicating slight to strong  
387 water repellency.



388 Soil respiration in biodegradation controls, namely non-sterile soils without phenolic compounds, was  
 389 16–38 mg kg<sup>-1</sup> C-CO<sub>2</sub>. Sterile, UV-irradiated controls ranged from 20 to 33 mg kg<sup>-1</sup> C-CO<sub>2</sub>  
 390 (supplementary material S6). Given prior sterilization, the photooxidation treatment generally respired  
 391 14–23 mg kg<sup>-1</sup> C-CO<sub>2</sub> less than the biodegradation treatment (Figure 4a). However, soil respiration of  
 392 each treatment did not change significantly within the course of the experiment as indicated by 95 % CI  
 393 testing.

394 The ergosterol content in biodegradation controls remained at 2.1–2.2 mg kg<sup>-1</sup> during incubation  
 395 (supplementary material S6). Sterile, UV-irradiated controls decreased from initial 1.04 ± 0.06 mg kg<sup>-1</sup>  
 396 to 0.34 ± 0.03 mg kg<sup>-1</sup> ergosterol towards the end of the experiment, which was mostly likely attributed  
 397 to UV-induced ergosterol degradation. By contrast, biodegradation of phenolic compounds significantly  
 398 increased the ergosterol content in soil by 3 ± 1 mg kg<sup>-1</sup> (95 % CI testing, Figure 4b).

399



400 *Figure 4: Differences in (a) soil respiration, (b) free ergosterol, and (c) PLFA biomarkers of microbial*  
 401 *groups in spiked soils with respect to non-spiked controls (zero line) at the first day (0) and last day (29)*  
 402 *of the incubation experiment; error bars indicate 95 % CIs; absolute numbers are given in the*  
 403 *supplementary material S6*

404

405 With respect to PLFA controls (see supplementary material S6 for detailed numbers), Gram-, Gram+,  
 406 and mycorrhiza biomarkers decreased by about 5 mol % during biodegradation of phenolic compounds  
 407 (Figure 4c). Consistent with ergosterol, fungal PLFA biomarkers strongly increased by 15 ± 6 mol %. In

408 the photooxidation treatment, changes in microbial biomarkers were mostly indistinct with respect to  
409 sample variation.

410 Accompanied by the increase in fungal PLFA and ergosterol biomarkers at day 29 of biodegradation, we  
411 observed extensive growth of fungal mycelia or fruiting bodies (sporocarp) in the incubation jars (see  
412 supplementary material S4 for images). This increase coincided with an increase in soil water repellency,  
413 which suggests that hydrophobic surface of fungal mycelia may have induced soil water repellency rather  
414 than photooxidation and polymerization of phenolic compounds as assumed by Tamimi et al. (2016).  
415 Owing to the fact that biomarker measurements were restricted to soil samples taken in the beginning  
416 and at the end of the experiment, it remains unresolved how the soil microbial community developed  
417 over time. Laor et al. (2011) reported a temporary increase in bacteria and fungi during the first 9 d after  
418 OMW application. In the following three months, bacterial counts decreased and fungi remained  
419 constant. The authors assumed bacteria to preferentially degrade easily available low-molecular-weight  
420 compounds while fungi took over for the degradation of more complex substances. However, in our  
421 study, soils were spiked only with low-molecular-weight phenolic compounds assumed to be easily  
422 available to microorganisms. It is therefore more likely that the initial treatment with phenolic compounds  
423 triggered rapid bacterial growth but that more slowly growing fungi eventually survived for their better  
424 adaptability to incubation conditions (Peikert et al., 2017). Additionally, phenolic compounds or  
425 temporarily present metabolites may have induced toxic effects towards bacteria rather than fungi  
426 (Capasso et al., 1995; Mekki et al., 2006). This could further explain why overall soil respiration  
427 remained constant at day 29 of biodegradation but was increased compared to controls and the  
428 photooxidation treatment as similarly observed by Peikert et al. (2017).

### 429 ***3.5. Discussion of degradation processes***

430 Soil biomarkers suggested that the biodegradation of phenolic model compounds was rather driven by  
431 fungal than by bacterial degradation. Biodegradation of phenolic compounds was further indicated to  
432 follow a pseudo-first-order reaction. Therefore, the reaction rate predominantly depended on the phenolic  
433 content. However, the pseudo-first-order reaction may have involved enzymatic catalysis or another  
434 reactant available in excess, for example oxygen. These findings are in contrast to those by Piotrowska  
435 et al. (2006) and Peikert et al. (2017) who found evidence for the development of suboxic soil conditions

436 attributed to the initial and rapid aerobic microbial degradation of phenolic compounds or other OMW  
437 constituents. But contrary to the experiment conducted by Peikert et al. (2017), our experimental design  
438 allowed explicitly for ambient air to be exchanged with the head space of the incubation jars. This  
439 suggests that the first rate-limiting step may have involved an oxidation reaction. If rate-limiting,  
440 oxidation of aromatic rings typically leads to AKIEs of 1.001–1.006 (Morasch et al., 2002; Vogt et al.,  
441 2008), which is comparable with the AKIE of  $1.007 \pm 0.002$  we observed for tyrosol. Moreover, our  
442 obtained AKIE was smaller than theoretically derived kinetic isotope effects of 1.01–1.03 for the  
443 oxidative cleavage of a C–H bond (Elsner et al., 2005). This further indicates that a non-fractionating,  
444 rate-determining step, such as mass transfer or substrate binding, must have preceded the catalytic bond  
445 cleavage involved in the oxidative biodegradation of tyrosol which masked the actual kinetic isotope  
446 effect (Elsner et al., 2012, 2005).

447 Although subject to high measurement uncertainty, biodegradation of vanillic acid indicated an AKIE of  
448  $0.987 \pm 0.005$ , and hence a depletion of  $^{13}\text{C}$ . Such an inverse isotope effect is interesting because natural  
449 degradation reactions typically enrich the parent compound in  $^{13}\text{C}$  rather than deplete it (Elsner et al.,  
450 2005). This deviation may be owed to the experimental design which included both vanillin and vanillic  
451 acid as phenolic model compounds. Vanillic acid is a common metabolite of vanillin (Neilson and Allard,  
452 2008). Consequently, the vanillic acid in the soil samples was of two origins: (1) the initial compound  
453 added through spiking and (2) the vanillin metabolite. Both vanillic acid species necessarily have a  
454 different isotopic composition, which renders the estimation of a reliable isotope enrichment factor  
455 impossible. This is a common problem when studying natural systems with a large number of potential  
456 compound sources and metabolic pathways. Similar observations were, for instance, made by Sherwood  
457 Lollar et al. (1999) and Maier et al. (2014), who studied the degradation of various aromatic compounds  
458 by native microbial communities without finding significant isotope effects.

459 Photooxidation of phenolic compounds was generally slower than biodegradation. Reaction kinetics were  
460 described equally well by zero- and first-order rate laws, which suggested the presence of another  
461 reactant, potentially a natural photocatalyst. This is consistent with the AKIE of  $1.02 \pm 0.01$  we observed  
462 for the photooxidation of tyrosol, and Zhang et al. (2016) found comparable AKIEs of 1.024 and 1.031  
463 for the hydroxyl radical-mediated photooxidation of nitrobenzene and dimethylaniline, respectively. By

464 contrast, photolytic bond cleavage is less likely to be the rate-limiting step of the degradation reaction,  
465 since it only induces AKIEs of 1.002–1.005 (Peng et al., 2013). The hydroxyl radicals required for  
466 photooxidation may have been formed by UV-induced photolysis of water with soil TiO<sub>2</sub> as photocatalyst  
467 (TiO<sub>2</sub>(h<sup>+</sup>) + H<sub>2</sub>O → TiO<sub>2</sub> + •OH + H<sup>+</sup>) or during photooxidation of SOM with reactive oxygen species  
468 (ROS) such as ozone or peroxides (ROS + SOM → SOM–HO•, Cheng et al., 2016).

469 Furthermore, Zhang et al. (2016) did not find any indication of compound polymerization during UV  
470 irradiation, which has been assumed to induce soil water repellency (Barbera et al., 2013; Tamimi et al.,  
471 2016). Here, we identified fungal growth during biodegradation of phenolic compounds as the main  
472 driver for soil water repellency.

#### 473 **4. Conclusions**

474 This pilot study investigated the feasibility of detecting changes in δ<sup>13</sup>C of selected phenolic compounds,  
475 namely tyrosol, vanillin, vanillic acid and coumaric acid, subjected to the sterile photooxidation and  
476 biodegradation by a native soil microbial community using compound-specific stable isotope analysis  
477 together with soil biomarkers. Our results suggested that biodegradation of phenolic compounds may has  
478 been dominated by fungi and most likely followed pseudo-first-order dissipation kinetics. Photooxidation  
479 was indicated to follow a mixed pseudo-zero- and first-order reaction probably mediated by hydroxyl  
480 radicals.

481 Although our newly developed GC–IRMS method performed well for laboratory standards, sample  
482 variation increased considerably when analyzing vanillin, vanillic acid, and coumaric acid in incubated  
483 soil. For tyrosol the method nonetheless allowed for distinguishing biodegradation and photooxidation  
484 by AKIEs and to discuss potential degradation mechanisms. In order to exploit the full potential of  
485 compound-specific stable isotope analysis, further method development should focus on reducing  
486 measurement variation which potentially originated from the heterogeneous structure of reaction spaces  
487 in soil. In such heterogeneous matrices, position-specific <sup>13</sup>C nuclear magnetic resonance or secondary  
488 ion mass spectrometry could help to better understand the nanoscale distribution and transformation of  
489 organic compounds. Once resolved, compound-specific stable isotope analysis could offer new  
490 opportunities for the identification of biotic and abiotic degradation processes of phenolic compounds in

491 the field. Such studies may then not be limited to plant residues but could extend to the analysis of  
492 allelochemicals exuded by roots or the characterization of lignin or SOM to derive a more comprehensive  
493 understanding of plant–soil interactions and SOM quality.

494

## 495 **Acknowledgments**

496 This study was part of TRILAT-OLIVEOIL (SCHA 849/13) and supported by the Ministerium für  
497 Wissenschaft, Weiterbildung und Kultur Rheinland-Pfalz, Germany, in the framework of the “Research  
498 initiative” program, project “AufLand”. We thank Kilian Kenngott and Jones Athai for fruitful  
499 discussions on the manuscript, Kevin Dolan for English editing as well as Silvia Eichhöfer and Andreas  
500 Hirsch for their help in the laboratory.

## 501 **Conflict of interests**

502 The authors declare no competing conflicts of interest.

- Barbera, A.C., Maucieri, C., Cavallaro, V., Ioppolo, A., Spagna, G., 2013. Effects of spreading olive mill wastewater on soil properties and crops: a review. *Agric. Water Manag.* 119, 43–53. <https://doi.org/10.1016/j.agwat.2012.12.009>
- Bisdorf, E.B.A., Dekker, L.W., Schoute, J.F.T.H., 1993. Water repellency of sieve fractions from sandy soils and relationships with organic material on soil structure. *Geoderma* 56, 105–118. [https://doi.org/10.1016/0016-7061\(93\)90103-R](https://doi.org/10.1016/0016-7061(93)90103-R)
- Bligh, E.G., Dyer, W.J., 1959. A Rapid Method of Total Lipid Extraction and Purification. *Can. J. Biochem. Physiol.* 37, 911–917. <https://doi.org/10.1139/o59-099>
- Blum, U., Shafer, S.R., 1988. Microbial populations and phenolic acids in soil. *Soil Biol. Biochem.* 20, 793–800. [https://doi.org/10.1016/0038-0717\(88\)90084-3](https://doi.org/10.1016/0038-0717(88)90084-3)
- Buchmann, C., Felten, A., Peikert, B., Muñoz, K., Bandow, N., Dag, A., Schaumann, G.E., 2015. Development of phytotoxicity and composition of a soil treated with olive mill wastewater (OMW): An incubation study. *Plant Soil* 386, 99–112. <https://doi.org/10.1007/s11104-014-2241-3>
- Butte, W., 1983. Rapid method for the determination of fatty acid profiles from fats and oils using trimethylsulphonium hydroxide for transesterification. *J. Chromatogr. A* 261, 142–145. [https://doi.org/10.1016/S0021-9673\(01\)87931-0](https://doi.org/10.1016/S0021-9673(01)87931-0)
- Campbell, C.D., Chapman, S.J., Cameron, C.M., Davidson, M.S., Potts, J.M., 2003. A Rapid Microtiter Plate Method To Measure Carbon Dioxide Evolved from Carbon Substrate Amendments so as To Determine the Physiological Profiles of Soil Microbial Communities by Using Whole Soil. *Appl. Environ. Microbiol.* 69, 3593–3599. <https://doi.org/10.1128/AEM.69.6.3593-3599.2003>
- Capasso, R., Evidente, A., Schivo, L., Orru, G., Marcialis, M. a., Cristinzio, G., 1995. Antibacterial polyphenols from olive oil mill waste waters. *J. Appl. Bacteriol.* 79, 393–398. <https://doi.org/10.1111/j.1365-2672.1995.tb03153.x>
- Cheng, M., Zeng, G., Huang, D., Lai, C., Xu, P., Zhang, C., Liu, Y., 2016. Hydroxyl radicals based advanced oxidation processes (AOPs) for remediation of soils contaminated with organic compounds: A review. *Chem. Eng. J.* 284, 582–598. <https://doi.org/10.1016/j.cej.2015.09.001>
- DIN 32645, 2008. Chemical analysis - Decision limit, detection limit and determination limit under repeatability conditions - Terms, methods, evaluation (Technical standard). Deutsches Institut für Normung, Berlin.
- Dungait, J.A.J., Stear, N.A., van Dongen, B.E., Bol, R., Evershed, R.P., 2008. Off-line pyrolysis and compound-specific stable carbon isotope analysis of lignin moieties: a new method for determining the fate of lignin residues in soil. *Rapid Commun. Mass Spectrom.* 22, 1631–1639. <https://doi.org/10.1002/rcm.3454>
- Elsner, M., 2010. Stable isotope fractionation to investigate natural transformation mechanisms of organic contaminants: principles, prospects and limitations. *J. Environ. Monit.* 12, 2005–2031. <https://doi.org/10.1039/C0EM00277A>
- Elsner, M., Jochmann, M.A., Hofstetter, T.B., Hunkeler, D., Bernstein, A., Schmidt, T.C., Schimmelmann, A., 2012. Current challenges in compound-specific stable isotope analysis of environmental organic contaminants. *Anal. Bioanal. Chem.* 403, 2471–2491. <https://doi.org/10.1007/s00216-011-5683-y>
- Elsner, M., Zwank, L., Hunkeler, D., Schwarzenbach, R.P., 2005. A New Concept Linking Observable Stable Isotope Fractionation to Transformation Pathways of Organic Pollutants. *Environ. Sci. Technol.* 39, 6896–6916. <https://doi.org/10.1021/es0504587>

- EN 14683, 2014. Medical face masks - Requirements and test methods (Technical standard).
- Gianfreda, L., Iamarino, G., Scelza, R., Rao, M.A., 2006. Oxidative catalysts for the transformation of phenolic pollutants: a brief review. *Biocatal. Biotransformation* 24, 177–187. <https://doi.org/10.1080/10242420500491938>
- Glaser, B., 2005. Compound-specific stable-isotope ( $\delta^{13}\text{C}$ ) analysis in soil science. *J. Plant Nutr. Soil Sci.* 168, 633–648. <https://doi.org/10.1002/jpln.200521794>
- Gong, P., Guan, X., Witter, E., 2001. A rapid method to extract ergosterol from soil by physical disruption. *Appl. Soil Ecol.* 17, 285–289. [https://doi.org/10.1016/S0929-1393\(01\)00141-X](https://doi.org/10.1016/S0929-1393(01)00141-X)
- Justino, C., Marques, A.G., Duarte, K.R., Duarte, A.C., Pereira, R., Rocha-Santos, T., Freitas, A.C., 2010. Degradation of phenols in olive oil mill wastewater by biological, enzymatic, and photo-Fenton oxidation. *Environ. Sci. Pollut. Res.* 17, 650–656. <https://doi.org/10.1007/s11356-009-0256-8>
- Kurtz, M.P., Peikert, B., Brühl, C., Dag, A., Zipori, I., Shoqeir, J.H., Schaumann, G.E., 2015. Effects of Olive Mill Wastewater on Soil Microarthropods and Soil Chemistry in Two Different Cultivation Scenarios in Israel and Palestinian Territories. *Agriculture* 5, 857–878. <https://doi.org/10.3390/agriculture5030857>
- Laor, Y., Saadi, I., Raviv, M., Medina, S., Erez-Reifen, D., Eizenberg, H., 2011. Land spreading of olive mill wastewater in Israel: Current knowledge, practical experience, and future research needs. *Isr. J. Plant Sci.* 59, 39–51. <https://doi.org/10.1560/IJPS.59.1.39>
- Lehmann, M.M., Gamarra, B., Kahmen, A., Siegwolf, R.T.W., Saurer, M., 2017. Oxygen isotope fractionations across individual leaf carbohydrates in grass and tree species:  $\delta^{18}\text{O}$  of individual leaf carbohydrates. *Plant Cell Environ.* 40, 1658–1670. <https://doi.org/10.1111/pce.12974>
- Maier, M.P., De Corte, S., Nitsche, S., Spaett, T., Boon, N., Elsner, M., 2014. C & N Isotope Analysis of Diclofenac to Distinguish Oxidative and Reductive Transformation and to Track Commercial Products. *Environ. Sci. Technol.* 48, 2312–2320. <https://doi.org/10.1021/es403214z>
- Meier-Augenstein, W., 1997. The chromatographic side of isotope ratio mass spectrometry: Pitfalls and answers. *LC GC* 15, 244–253.
- Mekki, A., Dhoub, A., Sayadi, S., 2006. Changes in microbial and soil properties following amendment with treated and untreated olive mill wastewater. *Microbiol. Res.* 161, 93–101. <https://doi.org/10.1016/j.micres.2005.06.001>
- Meyer, ArminH., Maier, MichaelP., Elsner, M., 2015. Protocol to Investigate Volatile Aromatic Hydrocarbon Degradation with Purge and Trap Coupled to a Gas Chromatograph/Isotope Ratio Mass Spectrometer. Humana Press, pp. 1–30. [https://doi.org/10.1007/8623\\_2015\\_174](https://doi.org/10.1007/8623_2015_174)
- Morasch, B., Richnow, H.H., Schink, B., Vieth, A., Meckenstock, R.U., 2002. Carbon and Hydrogen Stable Isotope Fractionation during Aerobic Bacterial Degradation of Aromatic Hydrocarbons. *Appl. Environ. Microbiol.* 68, 5191–5194. <https://doi.org/10.1128/AEM.68.10.5191-5194.2002>
- Neilson, A.H., Allard, A.-S., 2008. Environmental degradation and transformation of organic chemicals, Updated and expanded. ed. CRC Press/Taylor & Francis, Boca Raton.
- Peikert, B., Bibus, D., Fischer, J., Braun, U., Brunkhardt, J., Schaumann, G.E., 2017. Effects of olive oil mill wastewater on chemical, microbiological and physical properties of soil incubated under four different climatic conditions. *Biol. Fertil. Soils* 53, 89–102. <https://doi.org/10.1007/s00374-016-1157-x>

- Peikert, B., Schaumann, G.E., Keren, Y., Bukhanovsky, N., Borisover, M., Abo Garfha, M., Shoqeir Hasan, J., Dag, A., 2015. Characterization of topsoils subjected to poorly controlled olive oil mill wastewater pollution in West Bank and Israel. *Agric. Ecosyst. Environ.* 199, 176–189. <https://doi.org/10.1016/j.agee.2014.08.025>
- Peng, X., Li, X., Feng, L., 2013. Behavior of stable carbon isotope of phthalate acid esters during photolysis under ultraviolet irradiation. *Chemosphere* 92, 1557–1562. <https://doi.org/10.1016/j.chemosphere.2013.04.029>
- Piotrowska, A., Iamarino, G., Rao, M.A., Gianfreda, L., 2006. Short-term effects of olive mill waste water (OMW) on chemical and biochemical properties of a semiarid Mediterranean soil. *Soil Biol. Biochem.* 38, 600–610. <https://doi.org/10.1016/j.soilbio.2005.06.012>
- Reinnicke, S., Bernstein, A., Elsner, M., 2010. Small and Reproducible Isotope Effects during Methylation with Trimethylsulfonium Hydroxide (TMSH): A Convenient Derivatization Method for Isotope Analysis of Negatively Charged Molecules. *Anal. Chem.* 82, 2013–2019. <https://doi.org/10.1021/ac902750s>
- Rompa, M., Kremer, E., Zygmunt, B., 2004. Derivatization of Acidic Herbicides with Selected Tetraalkyl Ammonium and Trimethyl Sulfonium Hydroxides for Their GC Analysis. *Anal. Lett.* 37, 3299–3312. <https://doi.org/10.1081/AL-200040368>
- Schwarzenbach, R.P., Gschwend, P.M., Imboden, D.M., 2016. *Environmental Organic Chemistry*, 3rd ed. Wiley.
- Sherwood Lollar, B., Slater, G.F., Ahad, J., Sleep, B., Spivack, J., Brennan, M., MacKenzie, P., 1999. Contrasting carbon isotope fractionation during biodegradation of trichloroethylene and toluene: Implications for intrinsic bioremediation. *Org. Geochem.* 30, 813–820. [https://doi.org/10.1016/S0146-6380\(99\)00064-9](https://doi.org/10.1016/S0146-6380(99)00064-9)
- Sierra, J., Martí, E., Garau, M.A., Cruañas, R., 2007. Effects of the agronomic use of olive oil mill wastewater: Field experiment. *Sci. Total Environ.* 378, 90–94. <https://doi.org/10.1016/j.scitotenv.2007.01.009>
- Sierra, J., Martí, E., Montserrat, G., Cruañas, R., Aguilar, M.A., 2001. Characterisation and evolution of a soil affected by olive oil mill wastewater disposal. *Sci. Total Environ.* 279, 207–214. [https://doi.org/10.1016/S0048-9697\(01\)00783-5](https://doi.org/10.1016/S0048-9697(01)00783-5)
- Siqueira, J.O., Nair, M.G., Hammerschmidt, R., Safir, G.R., Putnam, A.R., 1991. Significance of phenolic compounds in plant-soil-microbial systems. *Crit. Rev. Plant Sci.* 10, 63–121. <https://doi.org/10.1080/07352689109382307>
- Steinmetz, Z., Kurtz, M.P., Dag, A., Zipori, I., Schaumann, G.E., 2015. The seasonal influence of olive mill wastewater applications on an orchard soil under semi-arid conditions. *J. Plant Nutr. Soil Sci.* 178, 641–648. <https://doi.org/10.1002/jpln.201400658>
- Tamimi, N., Diehl, D., Njoum, M., Marei, A., Schaumann, G.E., 2016. Effects of olive mill wastewater disposal on soil: Interaction mechanisms during different seasons. *J. Hydrol. Hydromech.* 64, 176–195. <https://doi.org/10.1515/johh-2016-0017>
- Vogt, C., Cyrus, E., Herklotz, I., Schlosser, D., Bahr, A., Herrmann, S., Richnow, H.-H., Fischer, A., 2008. Evaluation of Toluene Degradation Pathways by Two-Dimensional Stable Isotope Fractionation. *Environ. Sci. Technol.* 42, 7793–7800. <https://doi.org/10.1021/es8003415>
- Wheeler, M.W., Park, R.M., Bailer, A.J., 2006. Comparing median lethal concentration values using confidence interval overlap or ratio tests. *Environ. Toxicol. Chem.* 25, 1441–1444. <https://doi.org/10.1897/05-320R.1>
- Zelles, L., 1999. Fatty acid patterns of phospholipids and lipopolysaccharides in the characterisation of microbial communities in soil: a review. *Biol. Fertil. Soils* 29, 111–129. <https://doi.org/10.1007/s003740050533>



Zhang, N., Geronimo, I., Paneth, P., Schindelka, J., Schaefer, T., Herrmann, H., Vogt, C., Richnow, H.H., 2016. Analyzing sites of OH radical attack (ring vs. side chain) in oxidation of substituted benzenes via dual stable isotope analysis ( $\delta^{13}\text{C}$  and  $\delta^2\text{H}$ ). *Sci. Total Environ.* 542, Part A, 484–494. <https://doi.org/10.1016/j.scitotenv.2015.10.075>

This contribution was published as

Z. Steinmetz, M. P. Kurtz, J. P. Zubrod, A. H. Meyer, M. Elsner, G. E. Schaumann, *Biodegradation and photooxidation of phenolic compounds in soil – A compound-specific stable isotope approach*, *Chemosphere* 230 (2019) 230, 210-218” DOI: 10.1016/j.chemosphere.2019.05.030